ELSEVIER

Journal of Environmental Management 85 (2007) 628–637

Journal of Environmental Management

www.elsevier.com/locate/jenvman

Spatial scaling between leaf area index maps of different resolutions

Z. Jin[a,*], Q. Tian[a], J.M. Chen[b], M. Chen[b]

[a]International Institute for Earth System Science, Nanjing University, Nanjing 210093, China
[b]Department of Geography, University of Toronto, 100 St. George St., Room 5047, Toronto, Ont., Canada M5S 3G3

Received 4 August 2004; received in revised form 28 February 2006; accepted 9 August 2006
Available online 22 November 2006

Abstract

We developed algorithms for spatial scaling of leaf area index (LAI) using sub-pixel information. The study area is located near Liping County, Guizhou Province, in China. Methods for LAI spatial scaling were investigated on LAI images with 960 m resolution derived in two ways. LAI from distributed calculation (LAID) was derived using Landsat ETM + data (30 m), and LAI from lumped calculation (LAIL) was obtained from the coarse (960 m) resolution data derived through resampling the ETM + data. We found that lumped calculations can be considerably biased compared to the distributed (ETM +) case, suggesting that global and regional LAI maps can be biased if surface heterogeneity within the mapping resolution is ignored. Based on these results, we developed algorithms for removing the biases in lumped LAI maps using sub-pixel land cover-type information, and applied these to correct one coarse resolution LAI product which greatly improved its accuracy.
© 2006 Elsevier Ltd. All rights reserved.

Keywords: Remote sensing; LAI; Spatial scaling; Vegetation index; Sub-pixel

1. Introdoution

Remote sensing plays an important role in quantifying the spatial distribution of different surface parameters and, together with geographic information systems (GIS), increases the availability of data for use in various ecological models (Liu et al., 1997). Advanced satellite systems and sensors provide us with unique information that is critical to the modeling of natural phenomena at regional and global scales. Remote sensing provides the only way of observing global ecosystems consistently.

Various satellite sensors observe the Earth's surface at different spatial resolutions. In deriving surface parameters using remotely sensed data, the transportability of algorithms from one resolution to another is often of great concern because of the underlying surface heterogeneity. Inherent in the measurement approach, remote sensing yields average radiative signals from the sub-pixel elemental grid cells which usually consist of various land cover types. This signal-averaging process masks sub-pixel variations and consequently the averaged signals can induce biases when used to retrieve surface parameters, even if the same algorithms are used. Spatial scaling algorithms are therefore of great importance when remote sensing is applied to land ecosystems.

Two approaches may be employed in quantifying spatial heterogeneity. A textural approach based on the variability in brightness of pixels in an image uses many different parameters such as scale variance and variogram (Qi and Wu, 1996; Wu and Dennis, 2000; Atkinson et al.,1996; Hay et al., 1997) to define the spatial heterogeneity. More recently, a contextural approach has been developed that uses information about the size and shape of features displayed on an image including their areas, spatial distributions, and patterns (Chen, 1999). The former approach uses image texture (variance and covariance) to quantify surface heterogeneity (Hall et al., 1992; Friedl et al., 1995), while the latter considers the various cover types as sub-pixel information. The contexture-based approach (Chen, 1999) was found to be more effective in the LAI calculations, where the textural parameters

*Corresponding author. Department of Geography, University of Utah, 260 S. Central Campus Dr. Rm. 270, Salt Lake City, UT 84112-9155, USA. Tel.: 801 581 6419; fax: 801 581 8219.
E-mail address: zhenyu.jin@geog.utah.edu (Z. Jin).

0301-4797/$ - see front matter © 2006 Elsevier Ltd. All rights reserved.
doi:10.1016/j.jenvman.2006.08.016

provided just only an approximation for the scaling effect in the same study. In this article, an ETM+ image of Liping County was used to study the effect of spatial scaling of LAI at two different scales (30 m and 1 km) using the contextural approach. The objective of the study was to use the classification information of the fine resolution image (ETM+) to develop spatial scaling algorithms for LAI, and then apply the algorithm to correct a coarse resolution (MODIS) LAI product.

2. Remote sensing data preprocessing

2.1. Remote sensing image preprocessing

The study area is located near Liping County in southwestern China. It covers the area from approximately 25°44′ to 26°31′ N and 108°37′ to 109°31′ E (Fig. 1), with an altitude of about 600–800 m above the sea level. The remote sensing image used in this study was acquired by Landsat-7 ETM+ (Path/Row: 125/42) on May 14, 2000. Using the image header, we could ascertain that the imaging quality was high and there was no cloud. The surface reflectance values for three bands ETM3 (red), ETM4 (near infrared), and ETM5 (shortwave infrared) were used to derive various vegetation indices (VI). Two main steps of the remote sensing image preprocessing were implemented, atmospheric correction and geometric correction.

Hui and Tian (2003) demonstrated that atmospheric correction should be applied before using the vegetation indices to calculate LAI. In our case, the 6S model (Tanre et al., 1986) was used to correct the ETM+ image for atmospheric effects and to retrieve spectral reflectance at the surface level. Because many 6S parameters were not available at the time of image requisition, we selected the mid-latitude summer option to characterize the air mass during image acquisition.

The reason for the geometric correction was to match the ground LAI plots with the corresponding image pixels. To this end, 42 ground control points were located (mainly at

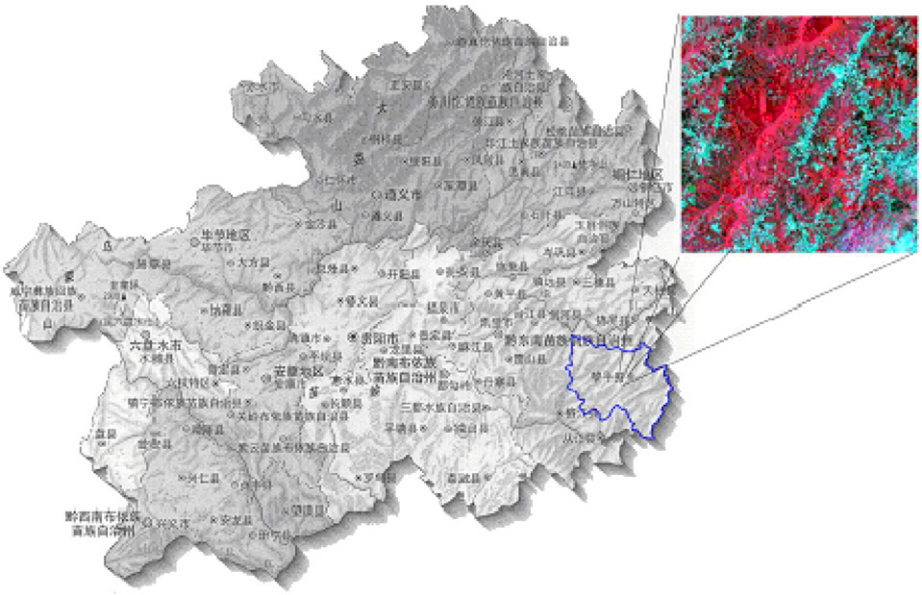

Fig. 1. A NIR-Red–Green composite of the Liping ETM+ scene.

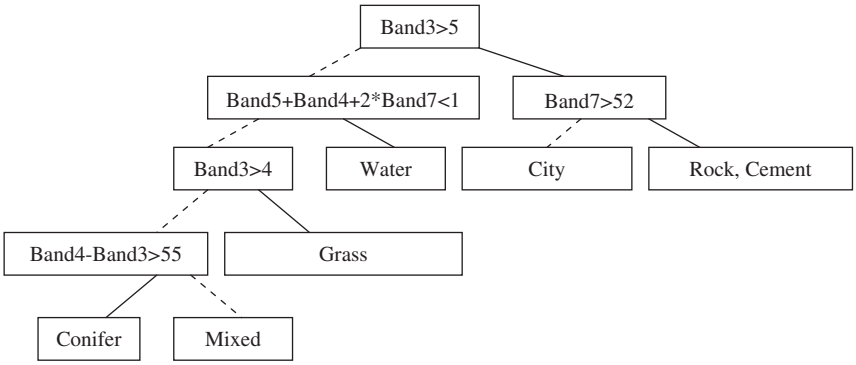

Fig. 2. Decision tree for ETM+ image classification.

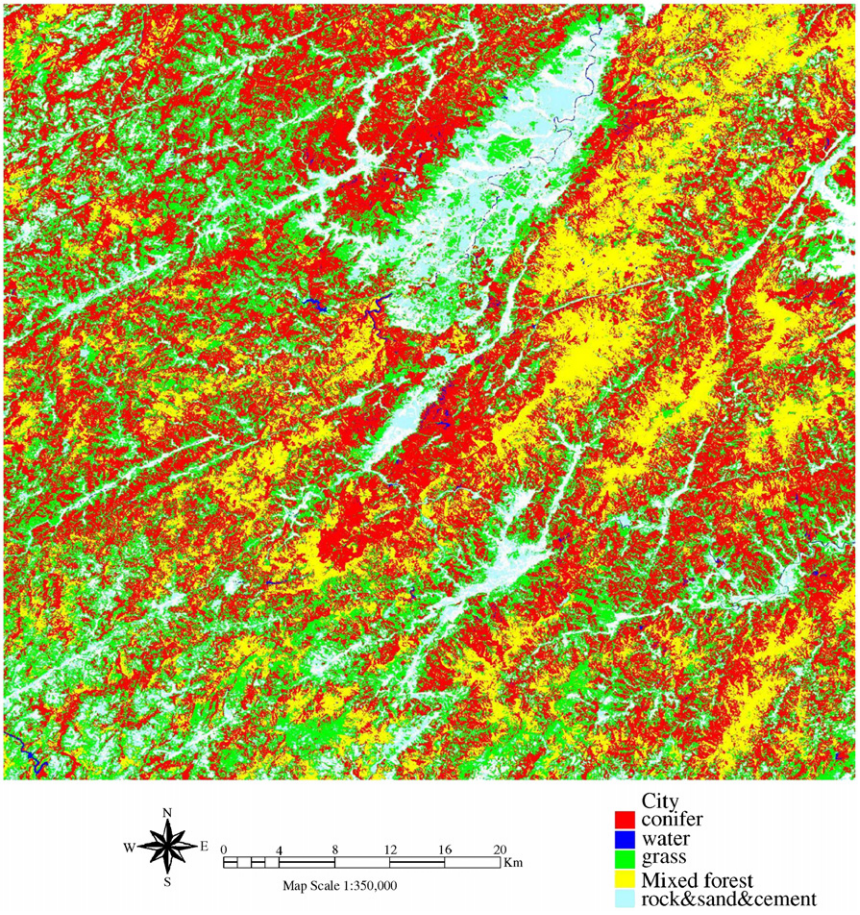

Fig. 3. The classified map of Liping ETM+ image.

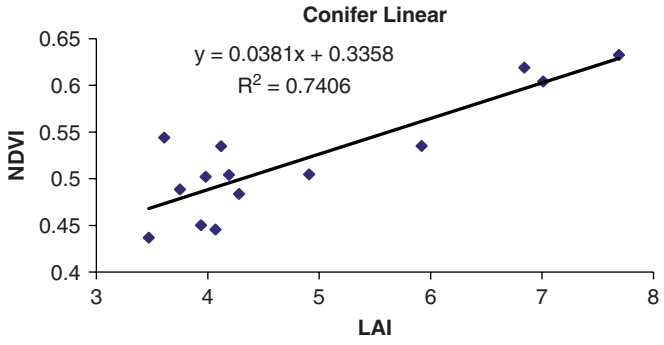

Fig. 4. Relationship of LAI–NDVI of conifer forest.

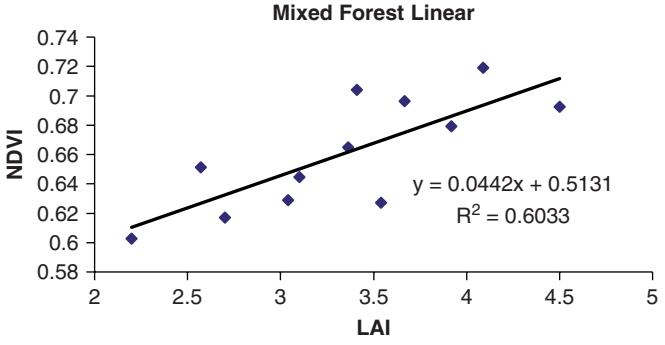

Fig. 5. Relationship of LAI–NDVI of mixed forest.

road crossings or river-road crossings) and used to geometrically rectify the ETM+ image with a root mean square error of 0.455 pixels.

2.2. Land cover types

Land cover information is crucial in quantifying surface parameters such as LAI. This is because different vegetation types have different canopy structure and therefore also exhibit differences in the absorption, reflection, and transmission of radiation. In addition, many biological parameters and variables such as LAI vary with vegetation type, thus correct land cover information is essential for quantifying such parameters.

In this study, we selected the decision tree method (Fig. 2) (Li and Ding, 2002) to classify the ETM+ image into 6 classes (Fig. 3). Conifers and mixed forest classes occupied about 38% and 20% respectively, with 42% of the land area belonging to other classes. Since broadleaf forest is not dominant in the study area and usually mixed or intermixed with conifers, it was incorporated into the mixed forest. Due to the absence of field measurements, we followed Chen et al. (2002), in combining grass, soil, city, cement, and some water into an "open land" category.

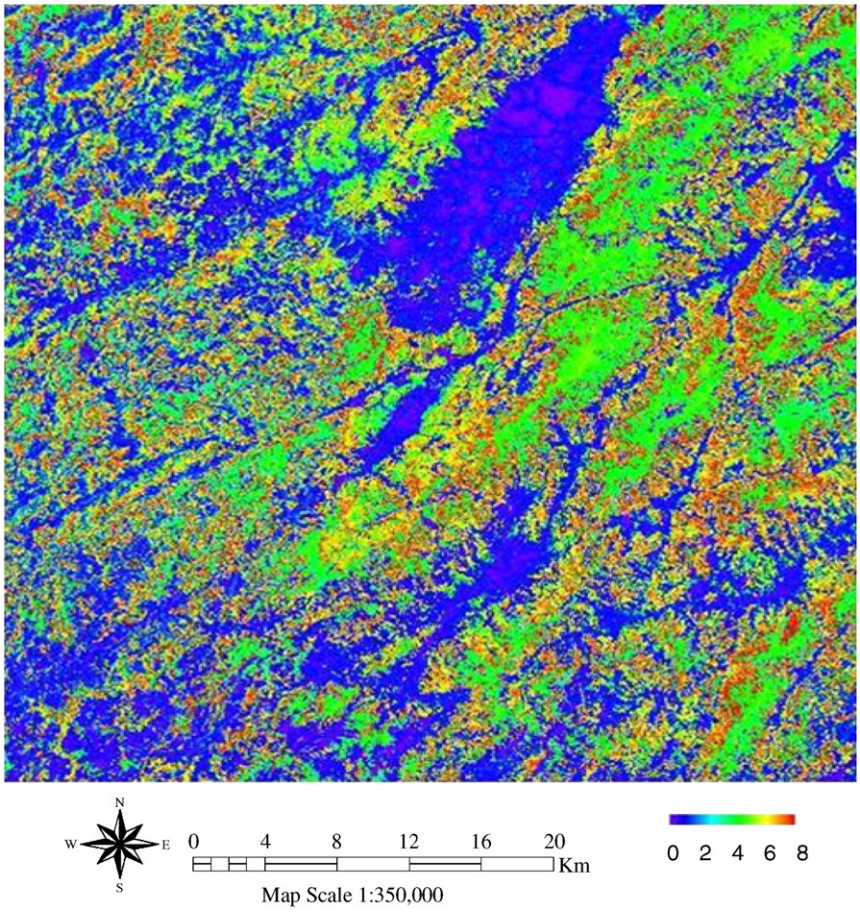

Fig. 6. ETM + LAI map of Liping county.

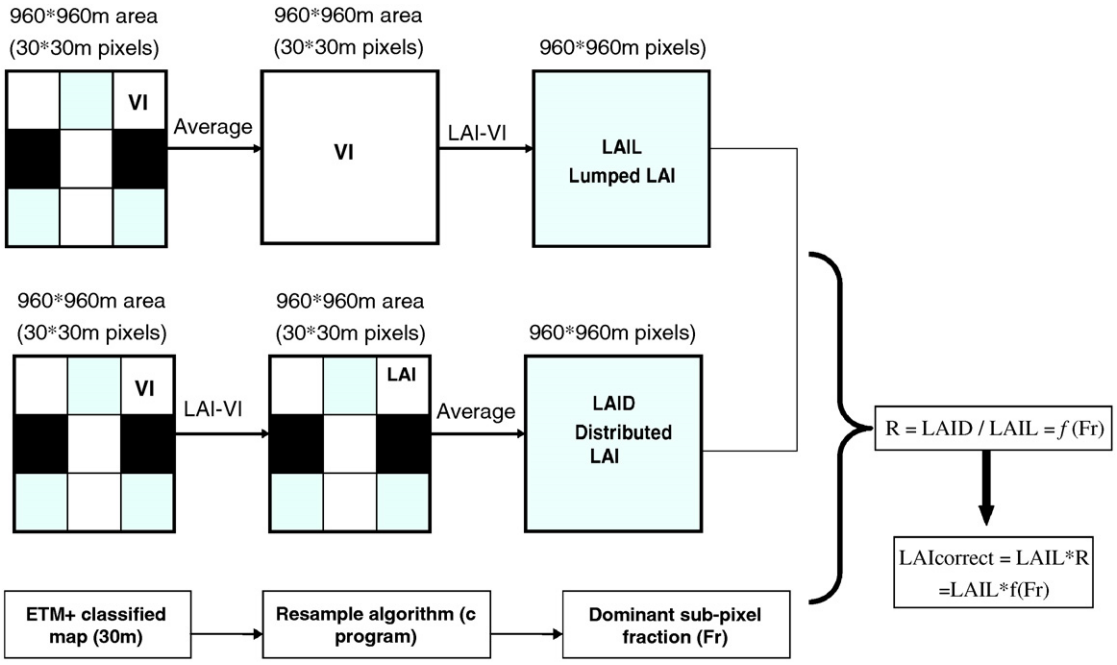

Fig. 7. Flow chart of spatial scaling methodology.

The open land also consists of different forms of natural landscape within the area of interest. It is defined as a land cover type consisting of recently burned areas, regenerated areas, and barren soil/rock and wetland areas. Although the LAI of water and city should be 0 or nearly zero, respectively, their areas were very small and the error caused by incorporating them into open land with non-zero LAI could therefore be ignored. In this study, the LAI-VI algorithm used for open land was adopted from Chen et al. (2002).

2.3. LAI mapping

LAI mapping was based on the LAI-VI relationship for the three vegetation types developed from ground LAI measurements. In August 2002, we used LAI (Pu and Gong, 2000) to measure about 30 plots of the coniferous and mixed forest, each plot approximately 150 m × 150 m or 5 × 5 pixels in the ETM+ image. In each plot, we made measurements at four locations and calculated the average LAI for the plot.

By using the absolute surface reflectance of the ETM+ image to produce NDVI and the reduced simple ratio (Chen et al., 2002), we built a linear regression model of VI against the field LAI measurements. Figs. 4 and 5 show the LAI-VI regression results for coniferous and mixed forests, respectively. Although we assumed a linear relation between LAI and NDVI which in this case is statistically significant, it should be noted that the relationship need not always be linear due to NDVI saturation level; depending on the type of vegetation cover, the saturation is reached asymptotically for LAI between 2 and 6. We could also see from Fig. 4 that the NDVI is approaching saturation when LAI is near 7–8 but, since we do not have enough LAI measurements in this range, a nonlinear model has not been chosen in this case.

Because no field LAI measurements were available for the open land, we used the LAI-RSR Eq. (2.1) developed by Chen et al. (2002).

$$\mathrm{LAI} = \mathrm{RSR}/1.3, \tag{2.1}$$

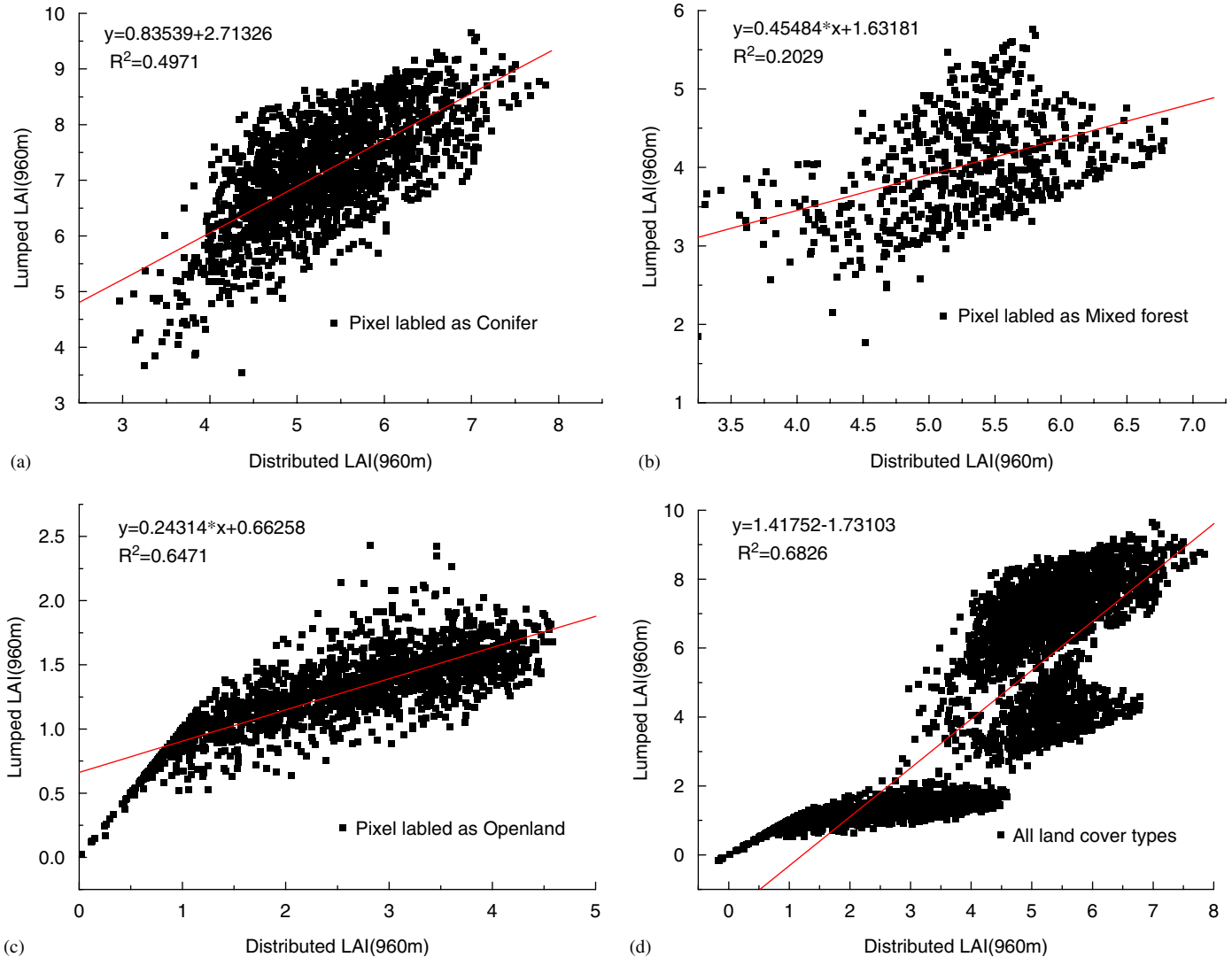

Fig. 8. Regression of uncorrected LAIL against LAID: (a) conifer, (b) mixed forest, (c) open land, and (d) all land cover.

where RSR is the reduced simple ratio defined based on red, NIR, and shortwave infrared reflectances.

Combining the three LAI-VI algorithms and the ETM+ classification, we produced the LAI map (Fig. 6) for Liping County using ENVI 3.5 remote sensing image processing software.

3. Spatial scaling model development

3.1. Products for spatial scaling

Methods for LAI spatial scaling were investigated using LAI images with 960 m pixels derived in two ways: (1) from distributed calculations (LAID), where LAID was calculated first at 30 m resolution and the averaged to 960 m resolution pixels; and (2) from lumped calculations (LAIL), in which LAI was calculated using input 30 m ETM+ vegetation index maps after resampling these to a resolution of 960 m. Fig. 7 shows the flowchart of spatial scaling steps.

3.2. Regression analysis of LAIL and LAID

Linear least-square regression analysis, with LAID as the independent variable, was used to investigate the relationship between LAID and LAIL (Fig. 8). Based on the lumped land cover map, each of the LAID and LAIL maps were separated according to the three cover types. The maps for the entire study area and for each land cover type separately were converted into ASCII files. The results are reported in terms of r^2 values. LAID is assumed to represent the reality; therefore, any deviation of LAIL from LAID is equivalent to the error produced in the coarse resolution LAI retrieval process.

Fig. 8 presents the correlation between uncorrected LAIL and LAID. For coniferous-labeled coarse resolution pixels, in view of the fact that the LAI is generally high for conifer forest, mixed pixels labeled as coniferous generally result in overestimation of LAIL, i.e. values are higher than those derived at fine resolution. Biases are also generally positive when pixels containing open water bodies are

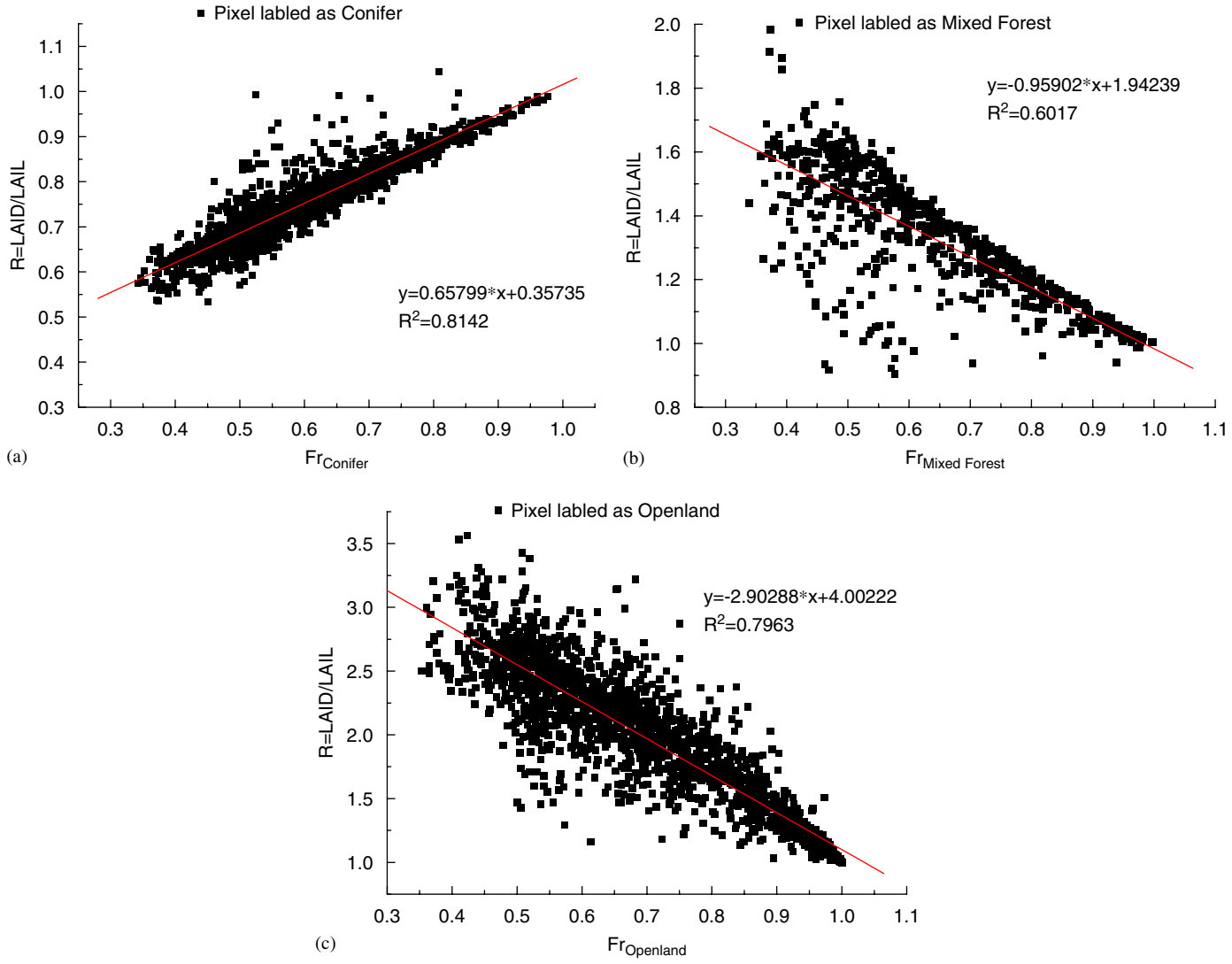

Fig. 9. Regression of correct factor against fraction: (a) conifer, (b) mixed forest, and (c) open land.

labeled as vegetation. In contrast, mixed pixels labeled as open land commonly have underestimated LAI values (Fig. 8c). In Fig. 8b, for the mixed forest-labeled coarse resolution pixels, overestimation of LAIL occurs when they contain significant fractions of conifers, while underestimation often occurs when they contain open land. It is thus evident that ignoring sub-pixel land cover-type information induces either positive or negative bias in LAI estimation. These biases depend on the dominant cover-type assigned to a lumped pixel (which is typically mixed). So the key part of the spatial scaling model development is to use sub-pixel land cover information to correct the LAIL.

3.3. Spatial scaling model

A C program was used to produce an ASCII file for cover-type area fractions within each 960 m pixel based on the known sub-pixel information from the 30 m resolution data. This step is most vital since the scaling algorithms could not be derived without the knowledge of cover-type area fractions (conifers, mixed forest, open land).

Since the goal of spatial scaling is to compute the LAI values from coarse resolution sensor data in such a manner that they equal the arithmetic average of the LAI values derived from fine resolution sensor data (Tian et al., 2002), the corrections of LAIL are based on the regression coefficients retrieved by correlating the correction factor R and each dominant cover-type fraction within the uniquely labeled coarse pixel. The relationships are as follows:

$$R = \mathrm{LAID}/\mathrm{LAIL}, \tag{3.1}$$

$$R_{\mathrm{type}} = a*\mathrm{Fr}_{\mathrm{type}} + b, \tag{3.2}$$

where $\mathrm{Fr}_{\mathrm{tyoe}}$ is the fraction of the dominant cover type; a, b are the linear regression coefficients for a particular dominant cover type.

Fig. 9 shows the relationships between the correction factor R and the dominant fraction within each lumped pixel. It is apparent that: (1) strong positive or negative

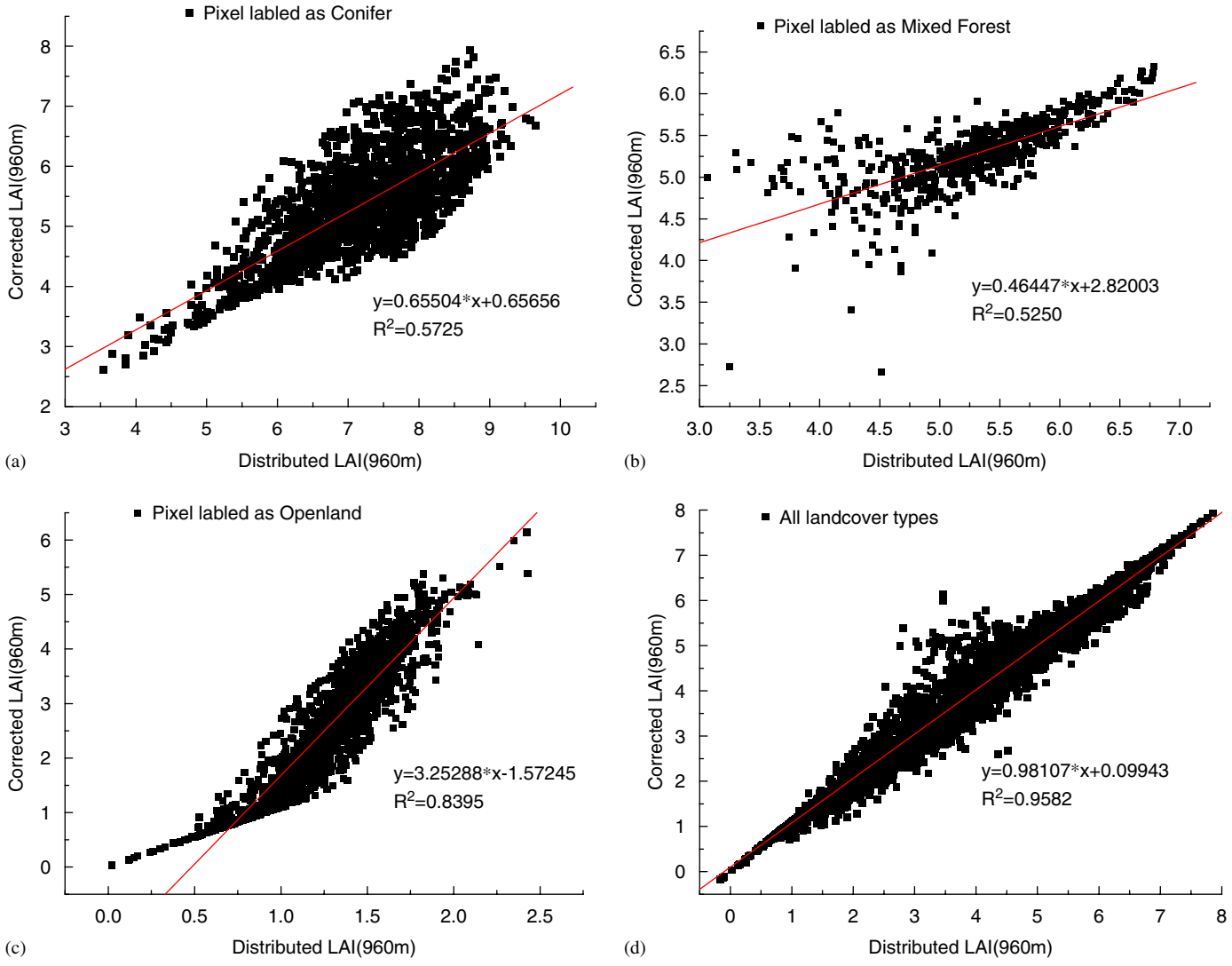

Fig. 10. Regression of corrected LAIL against LAID: (a) conifer, (b) mixed forest, (c) open land, and (d) all land cover.

linear correlations exist between R and Fr for the three cover types, so it is reasonable to develop the spatial scaling algorithm using cover-type area fractions; and (2) when Fr equals to 1, R equals to 1 as well. This proves that when using a linear LAI-VI algorithm, pure coarse resolution pixels will not cause differences between LAID and LAIL. The more pure a coarse resolution pixel is, the less error the LAIL will have.

According to the three equations in Fig. 9, we developed the spatial scaling algorithm (Eq. (3.3)):

$$\mathrm{LAI}_{\mathrm{correct}} = \mathrm{LAIL}*R = \mathrm{LAIL}*(a*\mathrm{Fr}_{\mathrm{type}} + b). \quad (3.3)$$

For conifers, mixed forest, and open land separately, the algorithms are, respectively, (3.4), (3.5), and (3.6):

$$\mathrm{LAI}_{\mathrm{correct}} = \mathrm{LAIL}*(0.65799*\mathrm{Fr}_{\mathrm{conifer}} + 0.35735), \quad (3.4)$$

$$\mathrm{LAI}_{\mathrm{correct}} = \mathrm{LAIL}*(-0.95902*\mathrm{Fr}_{\mathrm{mixedforest}} + 1.94239), \quad (3.5)$$

$$\mathrm{LAI}_{\mathrm{correct}} = \mathrm{LAIL}*(-2.90288*\mathrm{Fr}_{\mathrm{openland}} + 4.00222). \quad (3.6)$$

After using the three equations to correct the LAIL, we employed linear regression analysis to investigate the correlation between corrected LAIL and LAID (Fig. 10). It could readily be seen that after the corrections, the correlation between LAIL and LAID was much improved as the correlation increased from $R^2 = 0.68$ to $R^2 = 0.96$ for the entire image. For conifer-labeled coarse resolution pixels, the correlation increases from $R^2 = 0.50$ to $R^2 = 0.57$, for mixed forest-labeled coarse resolution pixels from $R^2 = 0.20$ to $R^2 = 0.53$, and for open land-labeled coarse resolution pixels from $R^2 = 0.65$ to $R^2 = 0.84$. These results demonstrate that the spatial scaling algorithms developed using sub-pixel information could greatly reduce the error in coarse resolution LAI mapping. Thus, if land cover-type information is available at high resolution, the above algorithms could be used to correct the coarse resolution (MODIS) LAI product.

To test our algorithm, we applied it to a subset of a MODIS LAI product produced by the University of Toronto, similar to that discussed by Liu et al. (1997). The corresponding ETM + image of the study area consists of 2048*2048 pixels. Figs. 11 and 12 show the correlations between MODIS LAI and LAID before and after correction, and Fig. 13 includes both original MODIS LAI map and the corrected map. From Figs. 11 and 12 it is evident that the linear correlation between corrected MODIS LAI and LAID was stronger than between uncorrected MODIS LAI and LAID. After the correction, the coefficient of determination R^2 increased from 0.54 to 0.79. The spatial scaling algorithm using sub-pixel information therefore significantly reduced the error in the MODIS LAI product. It also demonstrated that sub-pixel classification information for coarse resolution data is of great importance in the spatial scaling process.

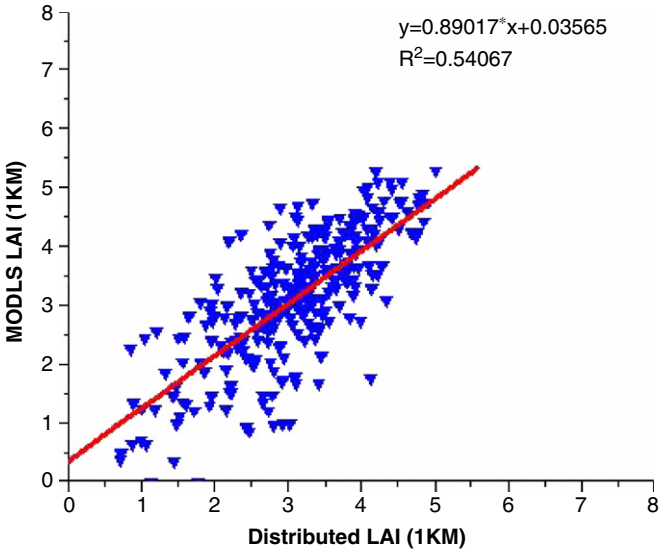

Fig. 11. Regression of uncorrected MODIS LAI against LAID.

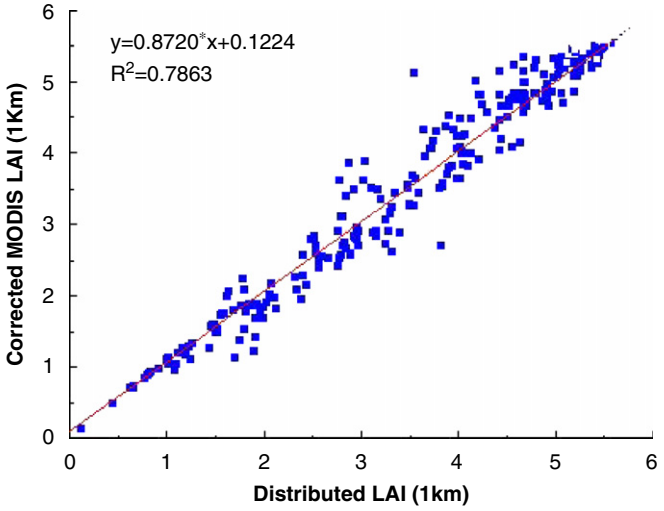

Fig. 12. Regression of corrected MODIS LAI and LAID.

4. Discussion

If only coarse resolution images are available for an area, a meaningful spatial scaling is severely limited. To meet the scaling requirement, the traditional practice in land classification based on "hard labeling" may be replaced with "soft labeling" approaches, i.e., giving the percentage of major cover types within each pixel. This soft classification approach has been successfully demonstrated by DeFries et al. (1997). However, it is generally difficult to apply the soft classification approach in case of multiple cover types through spectral unmixing, because the unique dimensions of optical remote sensing are generally smaller than the dimensions of surface variability (Verstrate et al., 1996). Therefore, greater attention should be paid to regional and global land cover mapping at high resolution.

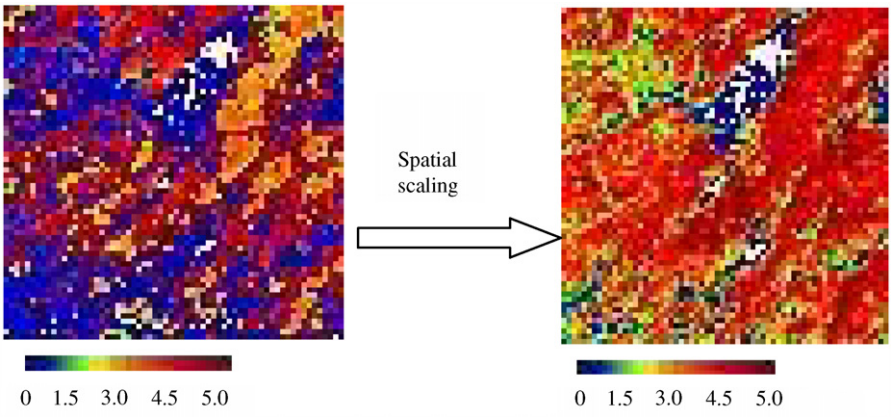

Fig. 13. Image of uncorrected MODIS LAI and corrected MODIS LAI (1 km).

This is in agreement with the suggestion by Chen (1999) that at least a high-resolution water area mask is required for spatial scaling of surface parameters.

Examples shown in this article are limited to two different scales and one biophysical parameter. However, the concept of scaling using contextural parameters could be applied in other surface parameters (such as FPAR, temperature, etc). In this study, only three types of vegetation are considered, and the coefficients determined in our scaling algorithm would be applicable to similar cover types in other regions. However, if we attempt to expand this method to other regions with different cover types, new sets of coefficients can be developed by following the examples given in this study.

5. Conclusions

Surface parameters derived at different spatial resolutions can be considerably different even though they are derived using the same algorithms, especially when coarse resolution pixels consist of various land cover types. In this study, we developed a spatial scaling algorithm for LAI between two scales (30 and 960 m) using a Landsat ETM + image of Liping County. The following main conclusions are drawn:

(1) Errors in coarse resolution LAI mapping occurred mainly because coarse resolution pixels are generally mixed and they are labeled as the dominant cover type in the LAI retrieval. LAI–NDVI relationships used in the LAI algorithm are inherently different among various structurally distinct cover types. This suggests that regional and global LAI maps produced without considering the sub-pixel vegetation-type variation would be in considerable error.
(2) An effective way of correcting errors in coarse resolution LAI images is to employ sub-pixel land cover information. It is demonstrated that when this information for three major cover types in Liping County was derived from a Landsat ETM + image at 30 m resolution and used to correct MODIS LAI at 1 km resolution, the error in the MODIS LAI was greatly reduced. This reduction in error was shown as a large increase in the correlation between the MODIS LAI and a high resolution LAI map derived using the ETM + image and ground data; the R^2 value increased from 0.54 to 0.79 after performing the correction using sub-pixel land cover fraction information. Our results demonstrate the need for high resolution land cover maps at regional and global scales for the purpose of accurate mapping of biophysical parameters which are land cover-dependent.

References

Atkinson, P.M., Dunn, R., Harrison, A.R., 1996. Measurement error in reflectance data and its implications for regularizing the variogram. International Journal of Remote Sensing 17, 3735–3750.

Chen, J.M., 1999. Spatial scaling of a remote sensed surface parameter by contexture. Remote Sensing Environment 69, 30–42.

Chen, J.M., Pavlic, G., Brown, L., Cihlar, J., Leblanc, S.G., White, H.P., Hall, R.J., Peddle, D.R., King, D.J., Trofymow, J.A., Swift, E., Van der Sanden, J., Pellikka, P.K.E., 2002. Derivation and validation of Canada-wide coarse-resolution leaf area index maps using high-resolution satellite imagery and ground measurements. Remote Sensing of Environment 80, 165–184.

DeFries, R., Hansen, M., Steininger, M., Dubayah, R., Sohlberg, R., Townshend, J., 1997. Sub-pixel forest cover in central Africa from multisensor, multitemporal data. Remote Sensing of Environment 60, 228–246.

Friedl, M.A., Davis, F.W., Michaelsen, D.J., Moritz, M.A., 1995. Scaling and uncertainty in the relationship between the NDVI and land surface biophysical variables: an analysis using a scene simulation model and data from FIFE. Remote Sensing of Environment 54, 233–246.

Hall, F.G., Huemmrich, K.F., Goetz, S.J., Sellers, P.J., Nickeson, J.E., 1992. Satellite remote sensing of surface energy balance: success, failures, and unresolved issues in FIFE. Journal of Geophysical Research 97 (D17), 19061–19089.

Hay, G.J., Niemann, K.O., Goodenough, D.G., 1997. Spatial thresholds, image-objects and upscaling: a multiscale evaluation. Remote Sensing of Environment 62, 1–19.

Hui, Feng-ming, Tian, Qing-jiu, 2003. Research and quantitative analysis of the correlation between vegetation and leaf area index. Remote Sensing Information 2, 10–13 (in Chinese).

Li, Yan, Ding, Sheng-yan, 2002. The decision tree classification and its application research in land cover [J]. Remote Sensing Technology and Application 17 (1), 6–11 (In Chinese).

Liu, J., Chen, J.M., Cihlar, J., Park, W.M., 1997. A process-based boreal ecosystem productivity simulator using remote sensing inputs. Remote Sensing of Environment 62, 158–175.

Pu, Rui-liang, Gong, Peng, 2000. Heperspectral Remote Sensing and it's Applications [M]. Higher Education Press, Beijing (in Chinese).

Qi, Y., Wu, J., 1996. Effects of changing spatial resolution on the results of landscape pattern analysis using spatial autocorrelation indices. Landscape Ecology 11, 39–49.

Tanre, D., Deroo, C., Duhaut, P., et al., 1986. The Second Simulation of the Satellite in the Solar Spectrum (6S) User Guide. UST.de Lille, France: L absoratoired' Optique Atmospherique.

Tian, Y., Woodcock, C.E., Wang, Y., Privette, J., Shabanov, N.V., Zhou, L., Zhang, Y., Buuermann, W., Dong, J., Veikkanen, B., Hame, T., Anderson, K., Ozdogan, M., Knyazikhin, Y., Myneni, R.B., 2002. Multiscale analysis and validation of the MODIS LAI product over Maun, Botswana. II. Sampling Strategy. Remote Senssing Environment 83 (3), 431–441.

Verstrate, M.M., Pinty, B., Myneni, R.B., 1996. Potential and limitations of information extraction on the terrestrial biosphere from satellite remote sensing. Remote Sensing of Environment 58, 201–214.

Wu, J., Dennis, E., 2000. Multiscale analysis of landscape heterogeneity: scale variance and pattern Metrics Jianguo. Geographic Information Science 6 (1), 6–19.